How Confinement Affects the Dynamics of C_{60} in Carbon Nanopeapods

S. Rols,[1,*] J. Cambedouzou,[2] M. Chorro,[2] H. Schober,[1] V. Agafonov,[3] P. Launois,[2] V. Davydov,[4] A. V. Rakhmanina,[4] H. Kataura,[5] and J.-L. Sauvajol[6]

[1]*Institut Laue Langevin, F-38042 Grenoble, France*
[2]*Laboratoire de Physique des Solides UMR 8502, Université Paris-Sud, F-91405 Orsay, France*
[3]*Laboratoire d'Electrodynamique des Matériaux Avancés, UMR CNRS-CEA 6157, F-37200 Tours, France*
[4]*Institute of High Pressure Physics of the RAS, R-142092 Troitsk, Moscow Region, Russian Federation*
[5]*Nanotechnology Research Institute, National Institute of Advanced Industrial Science (AIST), Central 4, Higashi1-1-1, Tsukuba 305-8562, Japan*
[6]*Laboratoire des Colloïdes, Verres et Nanomatériaux (UMR CNRS 5587), Université Montpellier II, F-34095 Montpellier Cedex 5, France*

(Received 24 December 2007; revised manuscript received 1 June 2008; published 8 August 2008)

The dynamics of confined systems is of major concern for both fundamental physics and applications. In this Letter, the dynamics of C_{60} fullerene molecules inside single walled carbon nanotubes is studied using inelastic neutron scattering. We identify the C_{60} vibrations and highlight their sensitivity to temperature. Moreover, a clear signature of rotational diffusion of the C_{60} is evidenced, which persists at lower temperature than in 3D bulk C_{60}. It is discussed in terms of confinement and of reduced dimensionality of the C_{60} chain.

DOI: 10.1103/PhysRevLett.101.065507 PACS numbers: 63.22.−m, 63.22.Gh, 64.70.kt

Nanopores, and among them carbon nanotubes [1], are ideally suited to host atoms or molecules, forming guest-host systems whose structure and thermodynamical properties are most original [2–4]. At a practical level, carbon nanotube-based guest-host systems have significant potential for chemical separation and sensing, and for targeted drug delivery [5,6]. Carbon nanopeapod (NPP) is one of these systems. It is formed of one-dimensional (1D) C_{60} fullerene chains confined inside the hollow core of single walled carbon nanotubes (SWNT) [7]. In its bulk solid state, C_{60} crystallizes into a face centered cubic structure at room temperature, and the molecules perform nearly free rotations about their center of mass [8,9]. Upon cooling, long range orientational order of the C_{60} molecules is achieved through a first order phase transition towards a simple cubic phase at $T \sim 260$ K. The ''free'' rotations are replaced by hindered rotations (librations) [10,11]. In this phase, the molecules are still jumping between two orientations [10] down to $Tg \simeq 85$ K, where the orientations are frozen. The situation is expected to be significantly different for the NPP where the C_{60} are confined inside SWNT. Recent theoretical papers have underlined the importance of the tube's diameter on the configuration of the C_{60} chain [12–14]. In particular, Verberck and Michel [13,14] calculated that the lowest energy configuration of the C_{60} inside the nanotube, is the ''pentagonal orientation'' (the nanotube's long axis crossing the center of two opposite pentagons at the C_{60}'s surface) for nanotubes having a diameter $D_t \leq 14$ Å, and the ''standard orientation'' (the nanotube's long axis crossing the center of two opposite double bonds at the C_{60}'s surface) for 14 Å $\leq D_t \leq 15.8$ Å. It is the goal of this Letter to shed light on the dynamics of the confined C_{60} molecules by combining inelastic neutron scattering and Raman data measured in a large temperature range.

A 900 mg peapod sample was prepared using the sublimation method [15] and was characterized by several techniques [15,16]. The powder contains large bundles with a narrow diameter distribution centered around 13.6 Å and a large filling ratio of ~80% [16]. In order to remove any trace of polymerized C_{60} inside the nanotubes and of hydrogenated adsorbed molecules, we systematically baked the sample at 300 °C under vacuum prior to the experiment. A 300 mg raw SWNT sample showing similar characteristics to the one obtained for the peapod sample was used as reference. Two sets of experiments were performed. The first set made use of the IN1BeF filter analyzer spectrometer at the Institut Laue Langevin (ILL) to measure the generalized density of states (GDOS) at high energy transfers. The other set of experiments was performed using the IN4C spectrometer with neutron incident wavelengths of 1.1, 1.8, and 2.2 Å to complete the measurements in the low and intermediate energy ranges. The measurements were performed at 10 K on both instruments and for peapods and nanotube samples. Additional measurements were performed in the temperature range [10; 300 K] on the IN4C spectrometer. The Raman data were collected at 50 K using a 488 nm incident laser radiation. The results obtained from the measurements are discussed in the light of calculations of the GDOS that we performed assuming a force field model detailed in [17]. All calculations were performed at 0 K in the ''crystal phase'' assuming a perfect orientational order of the C_{60} along the entire length of the tube. The calculations presented here are those in the ''pentagonal orientation'' of the inserted molecules, but several other orientations of the

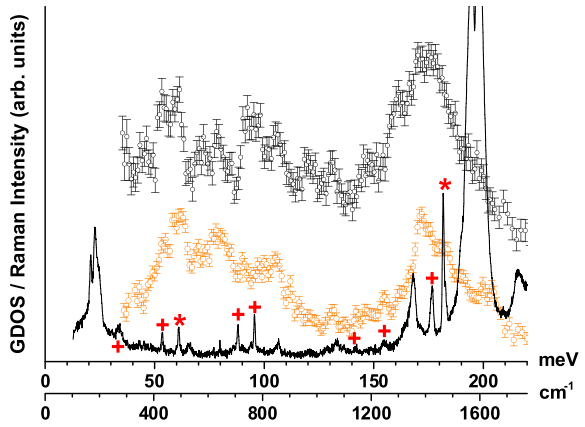

FIG. 1 (color online). Generalized density of states of the peapod sample (top spectrum) and of the SWNT sample (middle spectrum) measured at 10 K using the IN1BeF spectrometer compared with the Raman spectrum of the peapod sample (full line spectrum). The Raman active A_g and H_g modes are marked with a star and a cross symbol, respectively. Note that the Raman spectrum is plotted on a logarithmic scale for the y axis.

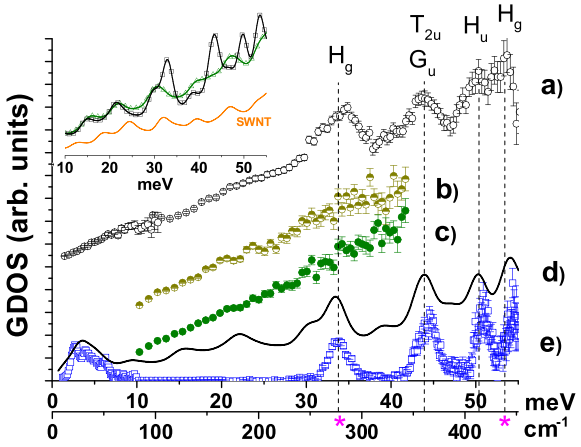

FIG. 2 (color online). Generalized density of states of the peapod sample measured on the IN4C spectrometer at 10 K (a), 150 K (b), 300 K (c), and the one calculated using the model developed in the text (d). The GDOS of a pure C_{60} sample measured at 10 K (e) is also shown for comparison. Inset: the GDOS calculated for a NPP model (squares and triangles) and for a SWNT model (labeled "SWNT," full line). The GDOS were folded with a Gaussian function (2 meV FWHM) to account for the instrument resolution. The curve with triangles symbols has its part originating from the C_{60} vibrations further folded with a Lorentzian having a FWHM of 6 meV to mimick the effect of the C_{60} rotations (see text).

C_{60} were tested. The calculated GDOS are broadened using a Gaussian linewidth of 2 meV (full width at half maximum—FWHM) to account for the spectrometer resolution.

Figure 1 shows the GDOS and the Raman spectrum of the peapod sample. They are compared to the GDOS of the SWNT sample. The Raman spectrum shows the dominant features originating from the tubes' resonant modes as well as additional peaks, the positions of which are in reasonable agreement with the Raman active modes for molecular C_{60}. This indicates a weak influence of the confinement on these modes, in agreement with previous Raman studies already published [18]. The nanotube GDOS has characteristic features that are rendered almost perfectly by the calculations that Ye *et al.* [19] performed on a (10,10) armchair nanotube using density functional theory (DFT). The peapods GDOS significantly differs from that of the SWNT. The C_{60} additional features modify the shape of the large band between 150 and 200 meV. Additional features are observed at 94, 121, and 148 meV. The low-frequency part of the spectrum (see also Fig. 2) shows a sequence of features at 33, 44, 50, and 53 meV that are in good correspondence with the H_g, G_u and T_{2u}, H_u and H_g C_{60} modes, respectively (see Fig. 2 and [20]). These latter features are very sensitive to the temperature : they progressively broaden to finally disappear into a sloping background upon warming up to 300 K (for clarity purposes, only the evolution of the H_g mode at 33 meV is presented on Fig. 2). Moreover, there is no clear signature of any libration mode of the confined C_{60} in the low-frequency part of the GDOS, by contrast to what is observed for C_{60} in its ordered phase and to what is predicted by the calculations.

Figure 3 represents the results of the low-frequency study of the NPP dynamics. Several representations are used on the same figure. First, the scattering function $S(Q, \omega)$ measured at 280 K is represented as a 2D graph using an appropriate color scheme (bottom right image). A signal appearing in the so-called *quasielastic* region, and having a strong Q dependence is clearly evidenced. The particularity of this signal stands in the two lobes centered on 3.4 and 5.5 $Å^{-1}$. Each of the spectra located at a fixed Q value can be fitted by the superposition of an elastic component (the delta function or the spectrometer function) and of a Lorentzian line shape modeling the quasielastic signal. The energy integrated intensity of the Lorentzian line is displayed in Fig. 3(c) (squares), where it is compared to the theoretical dependence calculated for a coherent quasielastic signal originating from "free" (isotropic) rotations of the C_{60} molecules [8,10,11], and from uniaxial 1D rotations of molecules in the pentagonal or standard orientations. The Q dependence of the experimental intensity seems in good agreement with all these models, the low quality of our data at high Q making a discrimination between them difficult. However, Michel and Verberck [13] predict that C_{60} pentagonal orientations in 13.6 Å peapods are separated by barriers that can be as small as 30 K (this is the energy difference between the standard and pentagon orientation). Therefore, "pseudo" isotropic rotations—implying more or less complex reorientations of the molecules around different axes—appear more likely. Moreover, one would expect oscillations of the

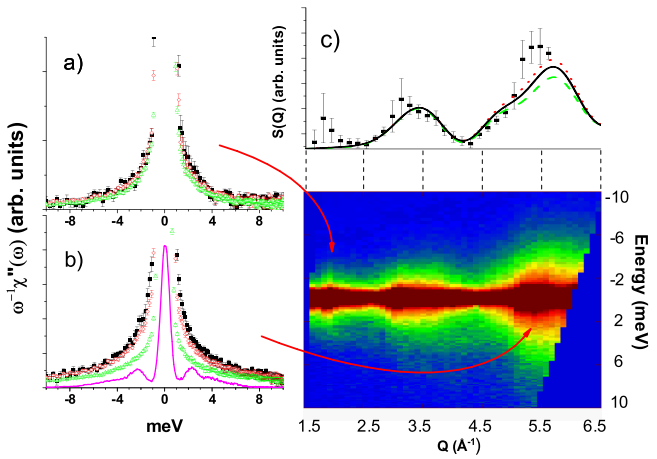

FIG. 3 (color online). Bottom right: the scattering function $S(Q, \omega)$ measured for the NPP sample at 280 K. Intensity is given by the classical thermal color scale. The intense elastic line centered at 0 meV is saturating the image (dark horizontal line). (a) and (b) Temperature dependence of the NPP susceptibility $\omega^{-1}\chi''(Q, \omega)$ (triangles = 200 K; circles = 100 K; squares = 50 K) measured at two wave vector transfers (a) $Q = 1.8$ Å^{-1}; (b) $Q = 5.4$ Å^{-1}). The susceptibility of "bulk" C_{60} is also drawn in (b) (bottom spectrum line, $T = 200$ K) showing the librations peaks at $\sim \pm 2.5$ meV. (c) Integrated intensity of the quasielastic signal measured at 280 K (squares) and calculated for a free rotation model of the C_{60} (full line) and for 1D rotation models in the pentagonal orientation (long dashes) and the standard orientation (dots).

molecules around axes perpendicular to the tubes in the case of 1D rotations. These would show up as librations bands in the inelastic region, in contrast to what is observed.

The relaxation nature of the signal can further be checked by correcting the scattering function for the thermal occupation. The corrected function is directly related to the imaginary part of the susceptibility $\chi''(Q, \omega)$ through the fluctuation-dissipation theorem: $S(Q, \omega) = \frac{1}{\pi}[1 - \exp(-\frac{\hbar\omega}{k_B T})]^{-1}\chi''(Q, \omega)$. In the following, we will use the convenient representation $\omega^{-1}\chi''(Q, \omega)$ and will often call this function *susceptibility* [21]. This representation is used in Figs. 3(a) and 3(b) for two different Q vectors: at $Q = 1.8$ Å^{-1}, the susceptibility measured at 50 K, 100 K, and 200 K are observed to superimpose, which is characteristic of a phononlike temperature dependence. At $Q = 5.4$ Å^{-1}, however, a clear jump is observed between the susceptibility measured at 200 K and those measured at 100 K and 50 K, the two last superimposing. The difference in the temperature dependence of the susceptibility at different Q can be explained by the fact that at low Q, the structure factor of the C_{60} rotation is very weak so that the signal measured is mainly originating from low-frequency excitations. These can be low lying radial deformation modes of carbon nanotubes and out-of-plane acoustic phonons from the graphitic impurities [16] present in the sample. In particular, the latter contribution is maximum in this Q range as the (0 0 2) diffraction peak of graphite is observed at 1.85 Å^{-1}. This is not the case at higher Q values where the quasifree rotations of the C_{60} molecules dominate the signal (see the two clear peaks in the structure factor located at 3.4 and 5.5 Å^{-1}) implying a nonbosonic T dependence in this Q range. At this point, it is necessary to emphasize that our data suggest that the C_{60} are performing fast diffusional reorientations at a temperature of 200 K, a temperature which is 60 K lower than the 260 K order-disorder transition temperature for cubic C_{60}. A clear change in the C_{60} dynamics occurs while lowering the temperature from 200 K down to 100 K. The boson-dependence of the intensity of the signal at $T \leq 100$ K suggests that the C_{60} rotation has lost its relaxation nature. This change in the dynamics can be made responsible for the drastic temperature dependence of the C_{60} vibrations. Under the assumption of a complete decoupling between the intramolecular modes of the C_{60} and their rigid-body rotations, the scattering function of the C_{60} intramolecular modes is the convolution of that of the rotations (i.e., a Lorentzian line shape) with a delta function (i.e., the spectrometer resolution function) centered at the frequency of the modes. To appreciate quantitatively this effect, the part of the numerical GDOS associated with the C_{60} vibrations was folded with a Lorentzian having a 6 meV FWHM. The value of 6 meV is the width of the quasielastic broadening measured using the 1.1 Å incident wavelength at 300 K. This value is consistent with the value of the quasielastic width at large Q values [11] measured for C_{60} in its disordered phase at the same temperature. The results of the calculation are presented in the inset of Fig. 2, where it is evident that the fast rotations make the sharp features from the fullerenes unobservable by merging them into the background originating essentially from the nanotube GDOS.

The main result from this study certainly stands in the surprisingly high orientational mobility of the C_{60} molecules -down to relatively low temperatures- when confined inside a nanotube. We already mentioned that these molecules undergo "free" rotations down to a transition temperature T_t which is much lower than its unconfined 3D equivalent of 260 K (100 K $\leq T_t \leq$ 200 K). Moreover, this transition is not followed by the appearance of intense and sharp inelastic features originating from librational modes like for 3D cubic C_{60} and characteristics of an orientational ordering. This implies that the transition is different in nature in each case. A possible scenario able to interpret the experimental data has to account for the specificity of the C_{60} when confined in a 13.6 Å diameter nanotube with a strong filling factor. Michel and Verberck [13,14] predict very small barrier for C_{60} reorientations inside 14 Å diameter tubes. Therefore, while the nanotube field restricts the center of mass position of the fullerenes

on a 1D chain along the nanotube axis, the molecular orientation of these molecules will be monitored by neighboring C_{60}-C_{60} interactions. This system can be described by a 1D-Ising type of model with nearest neighbor interactions between the C_{60} and with a static random field originating from the multitude of energetically very similar orientations of the C_{60} with regards to the host. In that picture, there is no proper ordering of the C_{60} at finite temperature, and the molecules can statistically adopt a large number of orientations. At low temperature, however, the weak but nonzero potential barrier that a C_{60} has to overcome to change from one orientation to another becomes non-negligible, and the molecules are pinned in various orientations in a time scale of the instrument resolution (i.e., in a ps time scale). Additional ingredients could be introduced in the model to give a more accurate description of the reduction of orientational mobility like the role of defects at the tube surface or the nonuniform filling of the tubes.

We have calculated that the librations of the C_{60} appear as well-defined features in the GDOS of a perfect crystal of peapods. However, its frequency is very sensitive to the orientation of the C_{60}, ranging from $\sim$0 up to 3.5 meV. A distribution of orientations results in a distribution of libration frequencies which would appear as a broad ''quasielastic-like'' signal. Its intensity would follow a Q dependence very similar to the one expected for free rotations (as it is the case for cubic C_{60} [10]). Moreover, any coupling with the low-frequency nanotube modes will further broaden the response of the librations. The absence of well-defined features associated to librations in the low-frequency region of the GDOS, even at the lowest temperature we considered (5 K), is somehow not surprising as far as a ''static'' orientational disorder of the C_{60} is considered. It is important to note that below 100 K, our data are unable to give more precise information about slower relaxations in this system. In particular, any reorientation of the C_{60} in a time scale larger than the picoseconds is out of reach. Additional experimental investigations, and, in particular, relaxation thermal measurements similar to those performed to study the glass transition in crystalline C_{60} [22], would be of great interest in order to shed light on the thermodynamic state of the confined fullerenes at low temperature.

In conclusion, we have used inelastic neutron scattering to probe the dynamics of NPP in a large energy and Q range. At a temperature of 10 K, the intramolecular modes of C_{60} are clearly observed for the first time and are in good agreement with what is expected from our calculations. At high temperature, a Q-dependent quasielastic signal is observed and attributed to rotations of the confined C_{60}. The temperature dependence of this signal shows a strong reduction of the orientational mobility of the C_{60} at a temperature $100\ \mathrm{K} \leq T_t \leq 200\ \mathrm{K}$, but the absence of well-defined libronic excitations at low temperature suggests a strong orientational disorder even at the lowest temperature reached (5 K). These results raise new questions both for experimentalists and theoreticians.

The authors acknowledge Dr. R. Almairac, Dr. L. Alvarez, and Dr. C. Goze-Bac for fruitful scientific discussions. This work benefited from the expert assistance of Dr. H. Mutka, Dr. J. Stride, and Dr. A. Ivanov during the neutron experiments.

Note added in proof.—Recently, the authors became aware of a NMR study on the C_{60} relaxations inside SWNT [23]. We recommend reading this article as a complement to our work.

*Also at Laboratoire des Colloïdes, Verres et Nanomatériaux (UMR CNRS 5587), Université Montpellier II, F-34095 Montpellier Cedex 5, France.

[1] *Understanding Carbon Nanotubes, from Basics to Application*, edited by A. Loiseau, P. Launois, P. Petit, S. Roche, and J.-P. Salvetat, Lect. Notes Phys. (Springer, New York, 2006).
[2] C. Cicero *et al.*, J. Am. Chem. Soc. **130**, 1871 (2008).
[3] B. Toudic *et al.*, Science **319**, 69 (2008).
[4] K. Shin *et al.*, Nat. Mater. 961 (2007).
[5] B. J. Hinds *et al.*, Science **303**, 62 (2004).
[6] L. Lacerda, A. Bianco, M. Prato, and K. Kostarelos, Adv. Drug Delivery Rev. **58**, 1460 (2006).
[7] B. W. Smith, M. Monthioux, and D. E. Luzzi, Nature (London) **396**, 323 (1998).
[8] D. A. Neumann *et al.*, Phys. Rev. Lett. **67**, 3808 (1991).
[9] P. Launois, S. Ravy, and R. Moret, Phys. Rev. B **52**, 5414 (1995); Int. J. Mod. Phys. B **13**, 253 (1999); S. L. Chaplot and L. Pintschovius, *ibid.* **13**, 217 (1999).
[10] J. R. D. Copley, W. I. F. David, and D. A. Neumann, Neutron news **4**, 20 (1993).
[11] B. Renker *et al.*, Z. Phys. B **90**, 325 (1993).
[12] M. Hodak and L. A. Girifalco, Phys. Rev. B **67**, 075419 (2003); H. Chadli *et al.*, *ibid.* **74**, 205412 (2006); K. S. Troche *et al.*, Nano Lett. **5**, 349 (2005).
[13] K. H. Michel, B. Verberck, and A. V. Nikolaev, Phys. Rev. Lett. **95**, 185506 (2005).
[14] B. Verberck and K. H. Michel, Phys. Rev. B **74**, 045421 (2006).
[15] H. Kataura *et al.*, Synth. Met. **121**, 1195 (2001).
[16] J. Cambedouzou *et al.*, Eur. Phys. J. B **42**, 31 (2004); Phys. Rev. B **71**, 041403(R) (2005).
[17] J. Cambedouzou *et al.*, Phys. Rev. B **71**, 041403(R) (2005).
[18] H. Kataura *et al.*, Appl. Phys. A: Mater. Sci. Process. **74**, 349 (2002).
[19] L.-H. Ye, B.-G. Liu, D.-S. Wang, and R. Han, Phys. Rev. B **69**, 235409 (2004).
[20] J. R. D. Copley, D. A. Neumann, and W. A. Kamitakahara, Can. J. Phys. **73**, 763 (1995).
[21] H. Schober *et al.*, Phys. Rev. B **56**, 5937 (1997).
[22] C. Meingast and F. Gugenberger, Mod. Phys. Lett. B **7**, 1703 (1993).
[23] K. Matsuda, Y. Maniwa , and H. Kataura, Phys. Rev. B **77**, 075421 (2008).